The effects of climate warming on large-scale atmospheric systems of the Northern Hemisphere

Zahra MAHAVARPOUR[1], Javad KHOSHHAL DASTJERDI[2]*,
Seyed Abolfazl MASOUDIAN[3] and Mohammad Ali NASRESFAHANI[4]**

[1] Ph.D. student, Faculty of Geographical Sciences and Planning, University of Isfahan, Isfahan, Iran.
[2] Associate Professor, Faculty of Geographical Sciences and Planning, University of Isfahan, Isfahan, Iran.
[3] Professor, Faculty of Geographical Sciences and Planning, University of Isfahan, Isfahan, Iran.
[4] Assistant Professor, Department of Water Resources Engineering, Faculty of Agriculture, University of Shahrekord, Chaharmahal and Bakhtiari, Shahrekord, Iran.
*Corresponding author: * j.khoshhal@geo.ui.ac.ir ; ** mnasr@sku.ac.ir

RESUMEN

En el presente estudio examinamos el impacto del calentamiento climático en la variabilidad de los principales impulsores climáticos en el hemisferio norte, utilizando 40 años (1979-2018) de datos de reanálisis de ERA-Interim. Para identificar regiones con variabilidad significativa de espesor de 500-1000 hPa, aplicamos el estimador de pendiente de Sen y la prueba de significancia de Mann-Kendall. Los hallazgos revelan que el calentamiento climático es particularmente pronunciado en latitudes que fluctúan entre 80º y 90º y también en regiones subtropicales. El aumento de espesor es más notable en las latitudes medias durante el verano, debido al calentamiento climático. La pendiente más pronunciada observada en otoño indica un ritmo de calentamiento más rápido en comparación con otras estaciones. A pesar del calentamiento climático, tendencias significativas en los sistemas de circulación atmosférica a gran escala demuestran el fortalecimiento de la alta presión siberiana en invierno y otoño; además, un segmento del núcleo del sistema de alta presión de las Azores también se fortalece durante el invierno. Por el contrario, los sistemas de baja presión del monzón y de las Aleutianas se debilitan en primavera e invierno, respectivamente. El sistema subtropical de alta presión exhibe una tendencia positiva y significativa en invierno, primavera y verano, alineándose con las tendencias positivas significativas observadas en el espesor atmosférico, lo cual confirma los efectos del calentamiento climático.

ABSTRACT

In the present study, we examine the impact of climate warming on the variability of the main climatic drivers in the northern hemisphere, using 40 years (1979-2018) of ERA-Interim reanalysis data. We applied Sen's slope estimator and the Mann-Kendall significance test to identify regions with significant variability of 500-1000 hPa thickness. The findings reveal that climate warming is particularly pronounced at latitudes ranging from 80º to 90º and also in subtropical regions. The increase in thickness is most notable in mid-latitudes during the summer season, owing to climate warming. The steeper trend slope observed in autumn indicates a faster warming rate compared to other seasons. Moreover, despite climate warming, significant trends in large-scale atmospheric circulation systems demonstrate the strengthening of the Siberian high-pressure in winter and autumn. Additionally, a segment of the core of the Azores high-pressure system has also experienced strengthening during winter. Conversely, the monsoon and Aleutian low-pressure systems have weakened in spring and winter, respectively. The subtropical high-pressure system exhibits a positive and significant trend in winter, spring, and summer, aligning with the positive significant trends observed in atmospheric thickness, thereby confirming the effects of climate warming.

Keywords: atmospheric thickness, climate warming, Mann-Kendall test, Sen's slope, significant trends.

1. Introduction

The impacts of imbalanced climate warming have led to abnormalities in meteorological parameters such as precipitation and temperature in various regions worldwide. If these abnormalities persist, they can be referred to as climate change. The variations in these parameters are primarily a result of significant alterations in atmospheric circulation patterns, particularly semi-permanent patterns. This is because the frequency, diversity, and intensity of pressure systems and atmospheric circulation patterns greatly influence the amplification of atmospheric conditions and climate components (Vicente-Serrano and López-Moreno, 2006). Therefore, investigating changes in key meteorological parameters like sea level pressure (SLP) is crucial for comprehending the intricacy of the climate system and the impact of anthropogenic warming on it (Patil et al., 2011). As a result, numerous studies have focused on this topic.

The main reason behind climate change is the radiative imbalance that leads to global temperature increase (Burt, 2005). Wallace et al. (2012), among others, stated that the changes in SLP during winter in the Northern Hemisphere were due to climate warming over the past few decades. As regions of cyclogenesis are connected to the quasi-permanent patterns of mid-latitudes and subtropical regions, any impact of climate warming on the meteorological variables in these specific regions will lead to climate anomalies in other areas. Consequently, numerous studies have examined these quasi-permanent weather systems individually in order to identify climate changes. For instance, Gong and Ho (2002), D'Arrigo et al. (2005), and Panagiotopoulos et al. (2005) documented a significant weakening of the Siberian high in the latter half of the 20th century. The most notable trend observed was a decrease of 2.5 hPa per decade from 1978 to 2001. Although they did not investigate the underlying dynamic factors, they emphasized that the weakening of the Siberian high should be considered a plausible outcome of climate warming. Moreover, they believed there is a strong negative correlation between long-term changes in the Siberian high and surface temperature.

Although the decrease in pressure trend is considered one possible outcome of climate warming, a study conducted by Jeong et al. (2011) reported a strengthening of the Siberian high during the period 1990-2010,

contradicting the findings of Panagiotopoulos et al. (2005). Falarz (2019) stated that the long-term trend at the center of the Azores high remained stagnant in June and increased by +0.63 hPa in January over each decade. He further noted that the reason is a reduction in air pressure difference between summer and winter. Using a linear model, Trenberth and Hurrell (1994) examined the Aleutian low-pressure system for a decade (1976-1988). They concluded that the deepening and eastward shift of the Aleutian low was associated with an increase in surface temperature in the Bering Sea. Lu et al. (2004) discussed that extratropical storm tracks play a role in modifying the wave associated with this low-pressure system, leading to a weakening of the Aleutian low. On the other hand, Xie et al. (2010), Deser et al. (2012) and Oshima et al. (2012) also believe that the relatively high atmospheric changes in the extratropical zone show a significant uncertainty in the intensity of the Aleutian Low's changes. Gan et al. (2016) demonstrated that this low-pressure system had strengthened during the 20th century. They applied a combined model approach to investigate the relationship between Arctic Sea ice melting and the Aleutian low, and projected that the Aleutian low would strengthen by –1.3 hPa and expand northward in the following century compared to the 20th century, as a result of climate warming.

Another form of quasi-permanent patterns is teleconnection patterns. Scholars such as Bjerknes (1968) and Horel and Wallace (1981) have pointed out the importance of teleconnection patterns in generating anomalies in atmospheric circulations in remote areas. A noteworthy instance can be the observed changes in the atmosphere and oceanic conditions of the tropical Pacific Ocean, which are transmitted to higher latitudes through teleconnection. Another example is the occurrence of monsoon lows, which are disturbances at the synoptic scale that form at the apex of the Bay of Bengal. These disturbances result in substantial rainfall but exhibit fewer extreme events (Sikka, 1977; Hurley and Boss, 2015; Hunt et al., 2016). The studies conducted by Sørland and Sorteberg (2015) and Dong et al. (2020) suggest climate warming has significantly reduced monsoon rainfall in central and northern India. This decrease can be attributed to the weakening of monsoon intensity and vorticity in the main core. Dong et al. (2017) argue that heavy rainfall events are closely linked to monsoon activity in the

main core. The decline in the number of heavy rainfalls in recent years may be attributed to the weakening of the monsoon low in the central core. Consequently, systems originating in the southern Bay of Bengal and the Arabian Sea have strengthened the primary system, leading to a general extension of monsoon rainfall beyond the north-central region of India.

Studies have also been conducted on the Mediterranean region. Maheras et al. (2001) demonstrated a decrease in the number of Mediterranean cyclones in the Western Mediterranean and an increase in their number in the Eastern Mediterranean from 1958 to 1977. Additionally, Trigo et al. (2000) stated that strong cyclones have been decreasing in the Western Mediterranean while weak cyclones have been increasing. While the current study focuses on pressure change trends rather than cyclones, it also examines the strengthening and weakening of pressure patterns as an indicator of cyclone intensity and changes in other climatic phenomena. The primary aim of the current study is to reveal the significance and the trend values for each main center of the pressure systems affecting the climate of the Northern Hemisphere, unlike the researchers who examined this issue regionally, including Gadedjisso-Tossou et al. (2021) in Togo, Frimpong et al. (2022) in Ghana, and Jiqin et al. (2023) in Ethiopia. However, most previous studies have primarily focused on specific regions, paying less attention to the overall integrated climate of the Northern Hemisphere.

Therefore, this paper examines the six activity centers or systems that play vital roles in the climate of the Northern Hemisphere, namely the Siberian, Azores, and Pacific highs, as well as the Icelandic, Aleutian, and Monsoon lows. Moreover, the Mediterranean SLP is considered a significant region for cyclogenesis and its impact on the climate of Eurasia is investigated. The quasi-permanent events discussed here are interconnected and should not be seen as isolated phenomena. One of the strengths of this research is the utilization of the non-parametric Mann-Kendall test to determine the trends in SLP, geopotential height of 500 hPa, and the 1000-500 hPa thickness across the entire Northern Hemisphere. The findings mainly concentrate on the changes in the permanent or quasi-permanent atmospheric patterns that dominate the Northern Hemisphere's climate. As a result, this study offers valuable insights to help readers better understand the effects of climate change on the climate of the Northern Hemisphere.

2. Study area
This research focuses on the large-scale atmospheric systems of the Northern Hemisphere. Considering the significant impact of these systems on the generation of various weather patterns and, consequently, the determination of the Northern Hemisphere's climate, a comprehensive examination of the entire hemisphere was undertaken. The deployment of the pressure systems has been determined according to the long-term average of 40 years of SLP. The location map of the studied pressure systems is illustrated in Figure 1.

3. Data and methods
In order to achieve the goals of the research, it is necessary to investigate the variability and its significance for the seasonal average of pressure in all regions of the Northern Hemisphere. For this purpose, data from the European Centre for Medium-Range Weather Forecasts (ECMWF) database were used
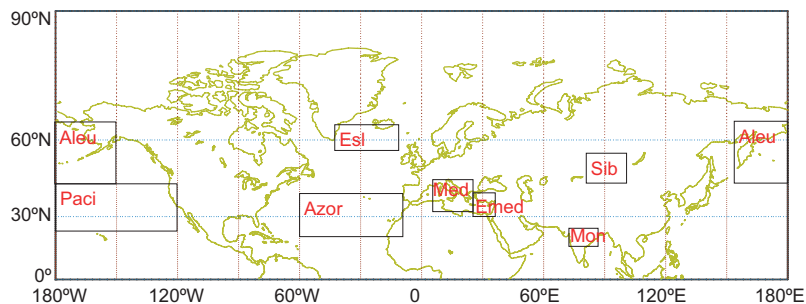

Fig. 1. General location of the studied pressure systems in the Northern Hemisphere.

from 1979 to 2018, including 14610 days for SLP, and 500 and 1000 hPa (geopotential height). The spatial resolution of the data is 1º in latitude and longitude, encompassing the entire Northern Hemisphere. The seasons are defined as follows: winter (January, February, and March), spring (April, May, and June), summer (July, August, and September), and autumn (October, November, and December). One of the parameters that can indicate climate warming and its impact on other meteorological parameters is the thickness of the atmosphere, which is directly related to the average temperature of the layer and increases/decreases with heating/cooling (NOAA/NWS, 2019). Meteorologists commonly use the 5400-m line to determine whether a region is cold enough for snowfall or warm enough for rainfall. This line separates polar streams from mid-latitudes (Hannigan and Godek, 2020). Therefore, thickness maps provide a direct representation of the temperature within the corresponding layer. In order to investigate the role of temperature in changes to pressure patterns, atmospheric thickness was calculated for all seasons.

The Mann-Kendall test was applied to examine the trend's significance at a 95% confidence level for SLP and 500 hPa at each grid point. The rate of changes was estimated using the Sen's slope estimator. By combining the Sen's slope map and Mann-Kendall significance, regions with positive or negative slope trends, both significant and insignificant, were identified in the Northern Hemisphere. To calculate the Mann-Kendall non-parametric test, the differences between the observations are first computed using S statistics (Eq. [1]).

$$s = \sum_{k=1}^{n-1} \sum_{j=k+1}^{n} sgn\left(x_j - x_k\right) \qquad j > k \qquad (1)$$

where n represents the total number of observations, while x_j and x_k denote the j_{th} and k_{th} values of the series. The resulting output of the aforementioned equation determines the symbol assigned to each series, as described by Eq. (2).

$$sgn(x) = \begin{cases} +1 & \text{if } \left(x_j - x_k\right) > 0 \\ 0 & \text{if } \left(x_j - x_k\right) = 0 \\ -1 & \text{if } \left(x_j - x_k\right) < 0 \end{cases} \qquad (2)$$

Then, the variance for each observation is calculated using Eq. (3).

$$VAR(S) = \frac{1}{18}\left[n(n-1)(2n+5) - \sum_{p-1}^{g} t_p\left(t_p - 1\right)\left(2t_p + 5\right) \right] \qquad (3)$$

where n represents the total number of observations, g the number of series containing at least one instance of duplicate data, and t the frequency of observations with identical values. The Z statistic is derived from the variance values and is calculated using Eq. (4) (Hirsch et al., 1982; Gibbons and Chakraborti, 2011).

$$\begin{cases} Z_{MK} = \frac{S-1}{\sqrt{VAR(S)}} & \text{if } S > 0 \\ Z_{MK} = 0 & \text{if } S = 0 \\ Z_{MK} = \frac{S+1}{\sqrt{VAR(S)}} & \text{if } S < 0 \end{cases} \qquad (4)$$

Finally, the null hypothesis is assessed in order to determine the presence or absence of a trend and its randomness. This hypothesis is approved when $-Z_{a/2} < Z < Z_{a/2}$ (Eq. [5]). The $Z_{a/2}$ values are the normal standard deviation (Z table) (Gan, 1998).

$$\left| Z \right| \leq Z_{a/2} \qquad (5)$$

In the present study, a significance level of $\alpha = 0.05$ was utilized. Considering the bilateral nature of the test, the Z value from the table was determined to be 1.96. Following the confirmation of the trend's significance, Sen's slope estimator was employed to calculate the rate of changes and its slope. This estimator is derived by computing the difference between the observations and their ranks, as demonstrated in Eq. (6).

$$Q = \frac{x_j - x_k}{j - k} \qquad (6)$$

where x_j and x_k represent the data observed in j and k times. The obtained median Q is equal to the slope of data time series (Banda et al., 2021).

4. Results and discussion

4.1 Trends in SLP and 500 hPa level changes in the Northern Hemisphere

This section provides the results obtained from analyzing the trends in SLP and the 500 hPa level.

Figure 2 illustrates the SLP pattern (Fig. 2a) and the height of the 500 hPa level (Fig. 2b). In Figure 2a, the subtropical high-pressure belt is clearly observable in the subtropical latitudes, as well as the Siberian high in North Asia. Additionally, the two low-pressure regions associated with the Atlantic-Pacific storm tracks are clearly depicted in the mid-latitudes over the Atlantic and Pacific. In Figure 2b, the dominant patterns are two deep troughs in the east of Asia and the Americas on the upstream of the Pacific and Atlantic storm tracks along with a weak and quasi-permanent trough in the Mediterranean.

4.1.1 Winter

Figure 3a demonstrates a significantly positive trend in SLP on the Pacific, known as the Pacific storm track. Notable changes in the 500 hPa level are predominantly observed in the polar and subtropical regions (Fig. 4a). By comparing the mean SLP map in Figure 2a with its trend map in Figure 3a, it is evident that the core of the Siberian high exhibits a positive trend ranging from 1.2 to 2.4 hPa over the 40-year period. The Azores high core

(Fig. 3a), is strengthened by 1.2 to 2 hPa during the 40-year period on a limited number of pixels. In the 500 hPa level (Fig. 4a), a significant positive trend in geopotential height is more extensively observed in the same area, with an increase of about 20 to 40 m over the 40-year period. No significant trends are observed in the northern area of the Atlantic, where the Icelandic low is located, in both studied levels (Figs. 3a, 4a). In winter, the most notable changes (Fig. 3a) belong to the Aleutian low. Figure 3a reveals that the core of the Aleutian low experiences a positive trend (increase in pressure) of up to 6.5 hPa at sea level, indicating its weakening. The results demonstrate that the trough associated with this low-pressure system is also weakened in the 500 hPa level, with an observed increase in height of up to 100 m above its core (Fig. 4a). The region spanning from the Southeast Pacific to the inner regions of Northern America also displays a positive trend of 2 to 4 hPa (Fig. 3a), indicating the strengthening of the high-pressure system in this region. The subtropical high near 30º N emerges as a prominent region, with a maximum height increase of 40 m (Fig. 4a).
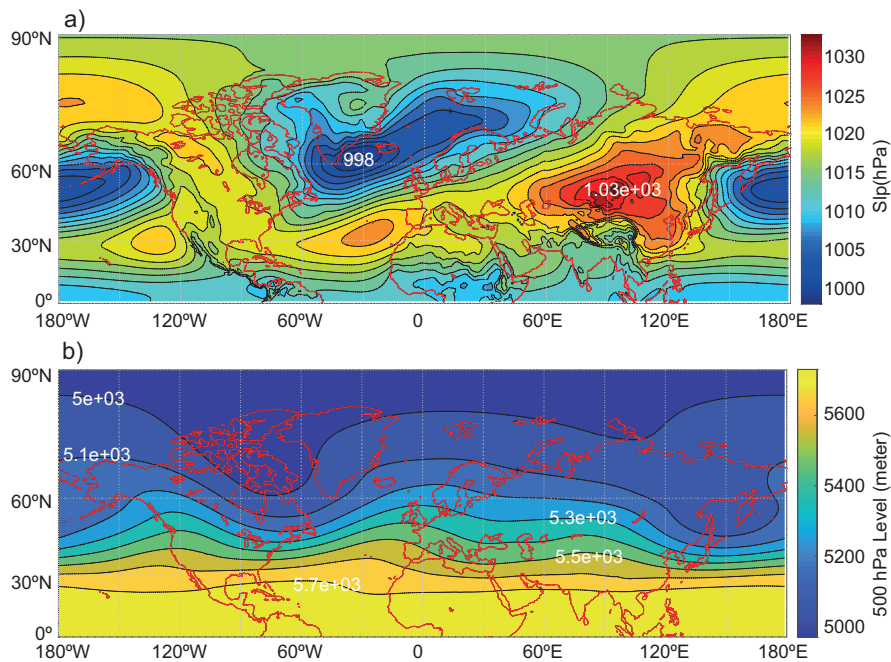

Fig. 2. (a) Long-term mean of sea level pressure (SLP) and (b) mean height of the 500 hPa level.
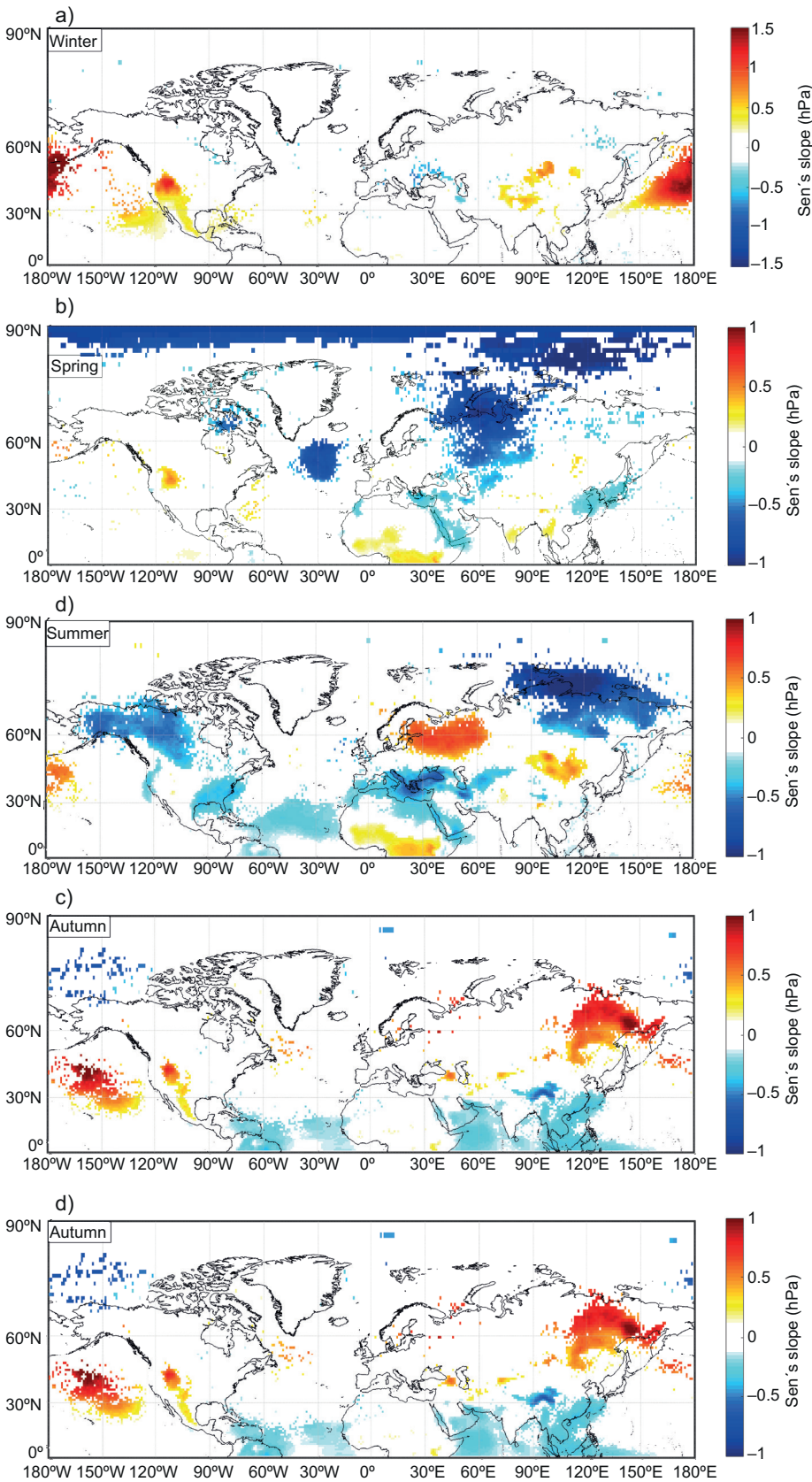
Fig. 3. Rate of SLP trends (hPa per decade^{-1}) for (a) winter, (b) spring, (c) summer, and (d) autumn. White areas do not exhibit any significant trends.
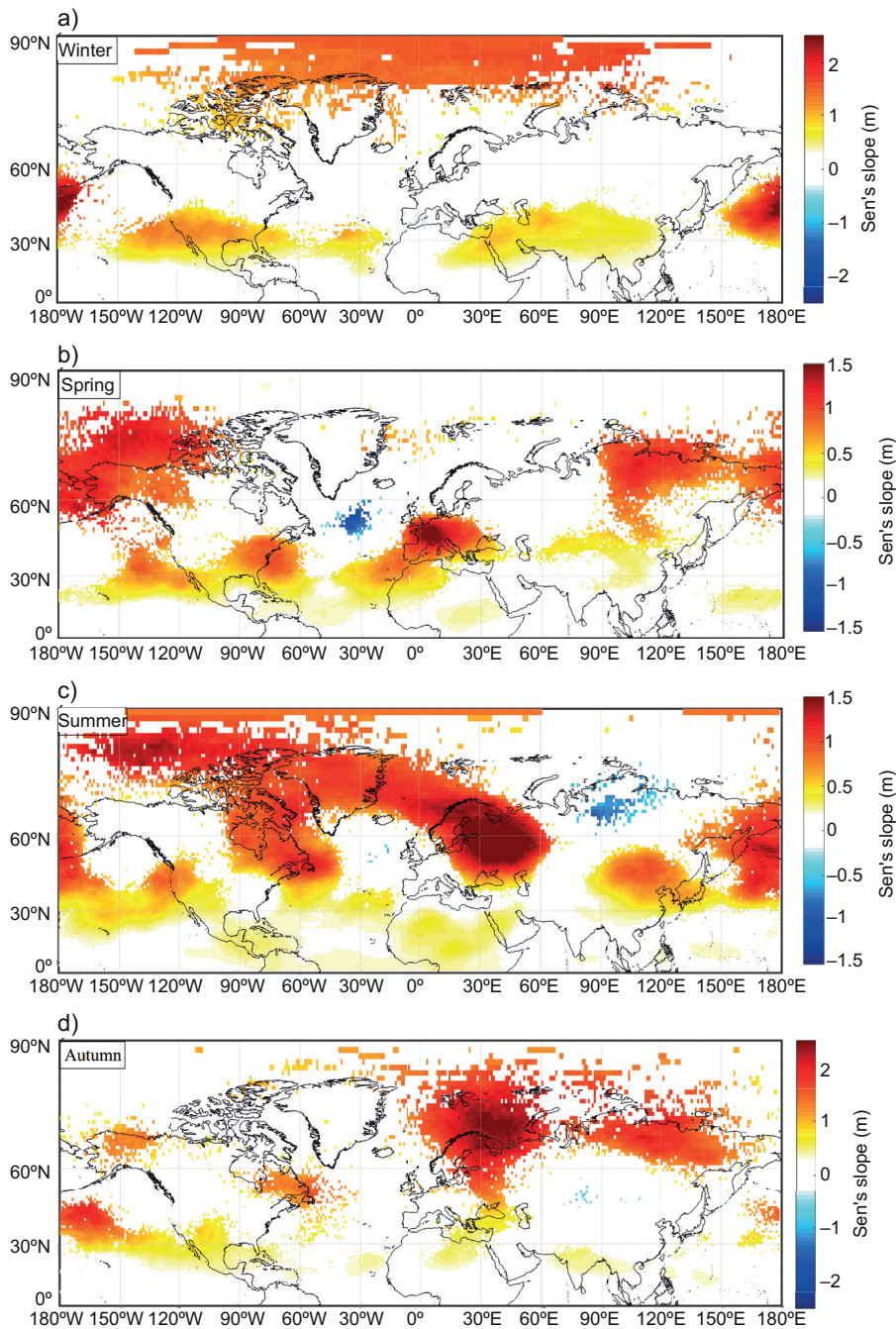
Fig. 4. Rate of 500 hPa level height trends (m year^{-1}) for (a) winter, (b) spring, (c) summer, and (d) autumn. White areas do not exhibit any significant trends

4.1.2 Spring

The monsoon low in its primary location (Fig. 1) in the northwestern Bay of Bengal exhibited a positive trend (weakening) of up to 0.5 hPa (Fig. 3b) over

a 40-year period. Figure 3b also depicts a negative trend and a decrease in pressure in the Red Sea and the eastern Mediterranean of up to –1.2 hPa during the same 40-year period. In spring, the Arctic region

(above 80º N), Western Siberia, and Eastern Europe demonstrate a prominent negative trend of –3.2 to –4 hPa (Fig. 3b) over the 40-year period. At the 500 hPa level (Fig. 4b), most regions in the Northern Hemisphere exhibit a significantly positive trend, with the exception of the central Atlantic region. Notably, there is a significant strengthening of the subtropical high by up to 20 m from West Africa to the East Pacific during the 40-year period, which can have an impact on the climate of a large part of the Northern Hemisphere. In the western Mediterranean at the 500 hPa level (Fig. 4b), a positive trend of 40 m was observed over the 40-year period. As mentioned earlier, a significant negative trend is observed in the sea and 500 hPa levels in the central Atlantic region, specifically between 50º to 60º N, known as the Atlantic storm track. Figure 3 shows a decrease in pressure to –3.2 hPa at the sea level (Fig. 3b) and a decrease in height to –40 m at the 500 hPa level (Fig. 4b) during the 40-year period, indicating a strengthening of the Atlantic storm track.

4.1.3 Summer

On the sea level trend map for summer (Fig. 3c), the Atlantic subtropical region exhibits a significant negative trend of –0.8 hPa, indicating a decrease in pressure. In the tropical regions of Central Africa, there is a pressure increase ranging from 0.8 to 1.6 hPa at sea level. Additionally, these regions experience a strengthening of the subtropical high at the 500 hPa level, with an increase in height ranging from 4 to 20 m (Fig. 4c). From 30º to 70º N in the Americas, there are two disconnected regions that show a significantly negative trend: one in the north, including northwest Canada and Alaska, with a trend of –1.6 hPa, and the other in the southeast with a trend of –0.8 hPa. The Red, Caspian, and Black seas, as well as the Mediterranean in West and Southwest Asia also exhibit a significantly negative trend, ranging from –0.8 to –2.4 hPa over the 40-year period. These trends suggest a warmer sea surface temperature (SST) and a heat low in the Middle East and Southwest Asia. Furthermore, Eastern Siberia experiences a significant negative trend of –1.4 to –4 hPa, indicating a decrease in pressure (Fig. 3c). At the 500 hPa level (Fig. 4c), there is a noteworthy strengthening of the ridge in northern Europe between 50º and 65º N, with an increase in height of up to 60 m over the 40-

year period. This strengthening is accompanied by a concurrent increase in pressure, reaching 2.4 hPa at sea level in this area (Fig. 3c). In the upstream regions of the storm tracks in the Atlantic and Pacific, significant increases in height can be observed, with an increase of up to 20 and 40 m over the 40-year period, respectively. In the subtropical region, where the strengthening of the subtropical high and its penetration towards higher latitudes are notable features in summer, a positive trend of 20 m can be observed over the 40-year period, particularly over land areas.

4.1.4 Autumn

During autumn, most regions do not exhibit a significant trend in terms of SLP, with the exception of Northeast Asia and the tropical regions of the Indian and Atlantic oceans (Fig. 3d). When the air gets colder in autumn, the Siberian high-pressure system becomes prominent on the map. This pressure system shows a positive trend, with its core pressure increasing by 4 hPa over a 40-year period. It is worth noting that there is an increase in pressure of up to about 4 hPa along the edge of the Siberian high and in Northeast Asia (East Siberia). At the 500 hPa level in this region (Fig. 4d), the height has increased by 40 to 60 m, indicating a strengthening of the ridge located downstream of the Pacific storm. The Mediterranean region does not show any significant trends at sea level (Fig. 3d), but its eastern part exhibits a positive trend of up to 20 meters in height at the 500 hPa level (Fig. 4d). In the map of the 500 hPa level (Fig. 4d), there is a pronounced and significantly positive trend between latitudes 60º to 80º N in North Europe during this season, indicating a weakening of the Icelandic low in this area.

4.2 Normality test and trend analysis of atmospheric thickness

To validate the trend analysis's results, a normality test was conducted using the Kolmogorov and Shapiro-Wilk methods on the spatial average of 1000-500 hPa thickness for all seasons. The results of this test are presented in Table I. Both methods indicate that the test is significant at a 95% confidence level. Additionally, the normality axis and Bell Curve Charts for all four seasons demonstrate that the data follows a normal distribution (Fig. 5).

After confirming the normality, the Mann-Kendall test and Sen's slope were conducted on the atmo-

Table I. Normality test of the four seasons at the 95 % significance level.

	Kolmogorov-Smirnov			Shapiro-Wilk		
	Statistic	DF	Significance	Statistic	DF	Significance
Winter	0.088	40	0.200*	0.957	40	0.137
Spring	0.045	40	0.200*	0.996	40	1.000
Summer	0.135	40	0.065	0.959	40	0.153
Autumn	0.126	40	0.113	0.964	40	0.235

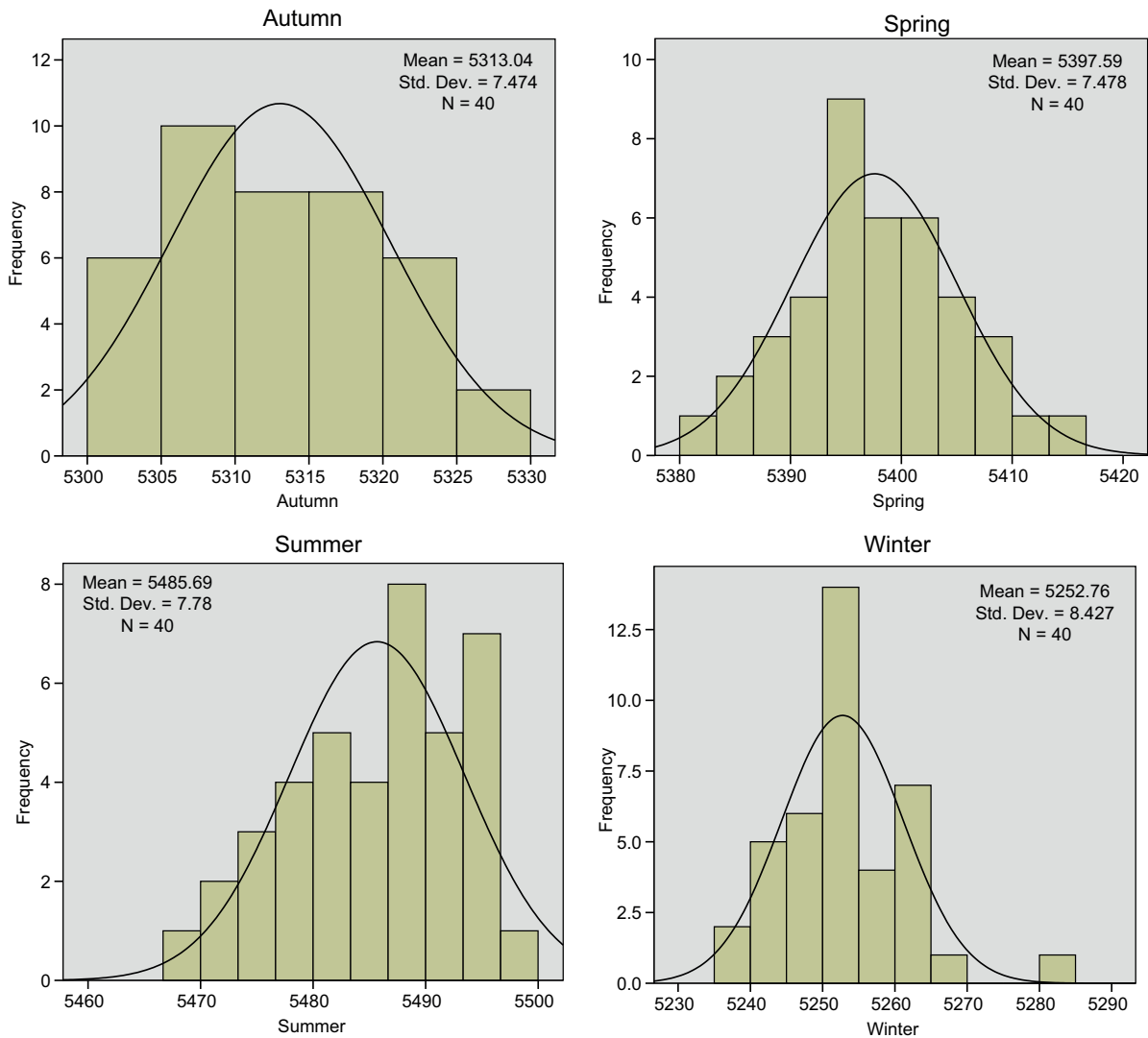DF: degrees of freedom; *Lower than true significance.

Fig. 5. Bell curve of normal distribution for each season.

spheric thickness data. Table II presents the results of Sen's slope calculation for each decade. The table reveals that the maximum increase in the height of the atmospheric thickness layer, or the highest positive trend of autumn, was approximately 5 m per decade, corresponding to a total increase of 20 m over the

Table II. Sen's Slope values of thickness in 500-1000 hPa per meter/decade (seasonal).

Winter	Spring	Summer	Autumn
4.613	4.81	4.776	4.951

40-year study period. In Figure 6, the seasonal diagrams of the trend and slope line, as well as the confirmation of the hypotheses of the regression model for atmospheric thickness, are presented. The characteristics of a well-performing linear regression model include normality, independence of variables, and the confirmation of the presence of variance. The quality of the regression is assessed through the residuals plot. The residuals should be randomly distributed around zero and should not exhibit any trends (Anscombe and Tukey, 2012). As demonstrated by the distribution method on the plots, all the initial assumptions of the model, including the normality
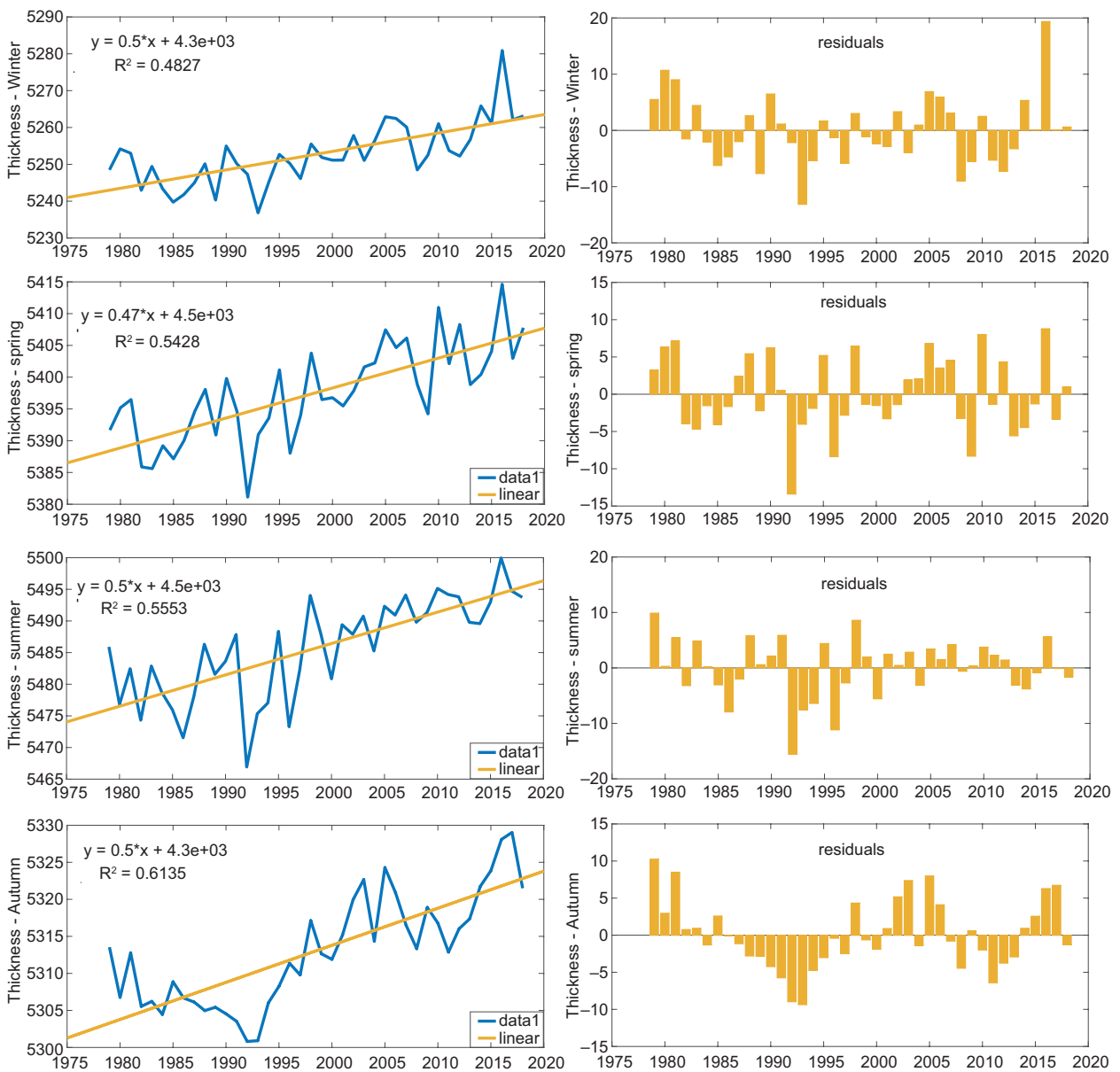

Fig. 6. Seasonal diagrams depicting the significance, Sen's slope (left panels), and residual plots (right panels).

assumption of the data, are correct. The significance test of the trend and Sen's slope approved strong and positive increase values in the atmospheric thickness in all seasons.

4.3 Thickness maps

The thickness maps of the atmosphere and the trends of their changes can be used to directly represent changes in atmospheric temperature. To evaluate the significance of the trends in atmospheric thickness changes, the test is conducted at a 95% significance level and Sen's slope value is calculated. Subsequently, maps are generated for the four seasons and compared to gain a better understanding of temperature variability in the Northern Hemisphere and the warming effects on the atmosphere, particularly in recent decades (see Fig. 7). Figure 7a displays the changes in thickness and their significance during the study period for the winter season. The greatest increase in atmospheric thickness is observed in the Polar Cap region. Notably, the subtropical regions around the 30º N latitude, particularly Southwest Asia to Northeast Africa, exhibit a significant increase of 10 to 30 m in thickness. The significant positive trend in atmospheric thickness in the Azores high-pressure region is consistent with the significant positive trend observed in SLP in this area (see Fig. 3a), although it does not cover a large area. The significant trend in atmospheric thickness has also weakened the Aleutian low. In other words, the Polar regions are warming at a faster rate compared to the tropical regions. The strong correspondence between Figures 7a and 4a clearly indicates the effects of climate warming on the Polar regions.

Figure 7b illustrates the variation in atmospheric thickness during the spring season. It is evident that there is a significant positive trend in the Northern Hemisphere, which has expanded to cover a larger area. It is worth noting that there is a decrease in atmospheric thickness in the North Atlantic region during this season, without any changes observed in winter. The map depicting the trend in thickness during the spring clearly indicates the impact of warming on the negative trend of SLP (Fig. 3b) between latitudes 80º to 90º N. Furthermore, the correspondence between Figures 7b and 4b indicates a direct relationship between significant positive trends at 500 hPa to 40 m and climate warming. This trend

occurred over a 40-year period, approximately ranging from 60º to 80º N, 100º to 180º E, 120º to 180º W, the Western Mediterranean, and the approximate range of subtropical high with a 20-m height increase (Fig. 4b). Figure 7c displays the results for the summer season, revealing that the most extensive regions experienced a significantly positive trend. In the Northern Hemisphere, except for parts of Eastern Asia and the east of the Atlantic, most regions show an increasing trend in atmospheric thickness over the 40-year period, indicating atmospheric warming. Additionally, Europe and East Asia stand out in the Northern Hemisphere with an approximately 50-m increase in thickness during this season. The greatest increase in atmospheric thickness occurs exclusively during autumn (Fig. 7d). The map illustrates a higher rate of warming during autumn. The results indicate that this increase is concentrated in the cold and Polar regions, particularly the Polar region of northern Eurasia, which has experienced an up to 20 m thickness increase per decade. The most substantial increase in thickness is observed in the polar region during this season, aligning with the reduction of ice cover in the Barents-Kara Sea (Yeager et al., 2015; Castruccio et al., 2019; Mori et al., 2019) and is the main source of the dramatic changes in the atmospheric circulation of the sub-polar latitudes (Semenov et al., 2009).

Numerous researchers have focused on the causes of polar ice surface reduction and have identified several factors (Kay et al., 2015; Swart et al., 2015; Gascard et al., 2019). According to Figure 7a, the thickness anomaly in autumn is centered on the Barents-Kara Sea and represents the most substantial thermal anomaly in the atmospheric column. In the Siberian high, the atmospheric thickness exhibits a decreasing trend of 4 m per decade, in line with the trend map of SLP increase for this high-pressure system in autumn. On the autumn thickness map, the significantly positive trends in the tropical region of the Atlantic, the Indian Ocean, and throughout the southern and southeastern coasts of Asia, in conjunction with the negative trends of –0.8 hPa (Fig. 3d), indicate decreased pressure resulting from higher warming in these regions during autumn. This heating in the subtropical zone during summer and autumn, however, leads to the expansion of the subtropical zone (Fu et al., 2006; Seidel and Randel, 2007) and
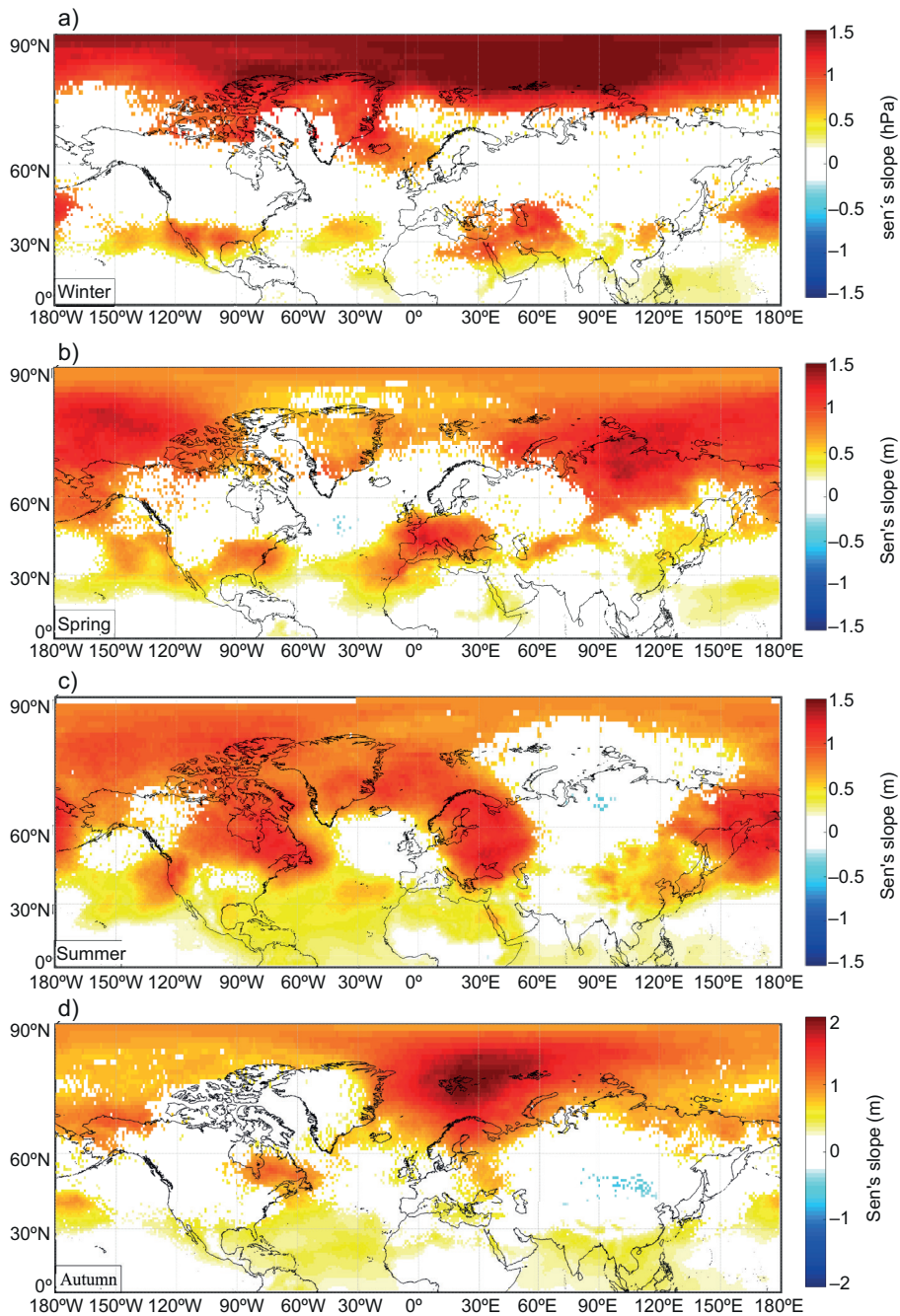
Fig. 7. Rate of atmospheric thickness 500-1000 hPa level (m year^{-1}) for (a) winter, (b) spring, (c) summer, and (d) autumn over 1979-2018.

the displacement of the subtropical jet stream towards the pole in the storm track region (Fu and Lin, 2011), which has an impact on the large-scale dynamics of the climate component of the Earth's atmosphere.

4.4 Analysis of major pressure centers
4.4.1 The Siberian high
The findings of this study indicate that the Siberian high-pressure system has strengthened as a result

of climate warming. Cohen and Entekhabi (1999) suggest that the decline in surface warming and atmospheric stability in Siberia, coupled with increased snow cover in Eurasia over the past two decades have contributed to this unexpected situation. These results contradict the research of Gong and Ho (2002) and Panagiotopoulos et al. (2005) but align with the findings of Jeong et al. (2011). Cohen et al. (2012) examined the physical processes underlying the strengthening of the Siberian high-pressure system in recent decades. They propose that the summer and autumn warming, along with increased humidity in high latitudes, leads to an increase in snow cover over Eurasia, which subsequently causes widespread cooling during winter. Mori et al. (2014, 2019) have also extensively discussed this issue, concluding that reduced sea ice in the Barents-Kara Sea is responsible for the occurrence of severe cold winters in Eurasia. The decrease in sea ice triggers multiple blocking events in Eurasia, resulting in the advection of cold air and the exacerbation of winter conditions. Semenov et al. (2009) have confirmed the nonlinear relationship between the reduction of polar ice in the Barents-Kara Sea and atmospheric circulations, particularly the anomalous anticyclone circulation, which induces a negative SST anomaly in central Eurasia. Throughout the Eurasian region and across all seasons, a decrease in atmospheric thickness (although not statistically significant) is observed, corroborating the occurrence of transient cold air outbreaks associated with numerous blocking events. A positive significant trend of the 500 hPa height level in the summer and autumn exactly in the contentious area of the Barents-Kara Sea has resulted partly in the deterioration of the ice cover due to climate warming, especially in late summer and early autumn (IPCC, 2021).

4.4.2 North Atlantic Ocean

The North Atlantic is influenced by two permanent pressure systems: the Azores high-pressure system in the subtropical region and the Iceland low-pressure system in the northern region. The teleconnection between these two systems, known as the North Atlantic Oscillation (NAO), regulates the behavior of the Atlantic storm track. Any changes in the intensity of the Azores high-pressure and the Iceland low-pressure systems in the North Atlantic region will result in a corresponding change in the NAO, which is the primary mode of atmospheric variability in the Northern Hemisphere. Therefore, the impact of climate warming on this region must be considered from these three aspects. Regarding the high-pressure Azores system at the 500 hPa level (subtropical high) and the atmospheric thickness within the same range, the significant positive trend observed aligns with the map of significant positive trends in atmospheric thickness, providing evidence of the effects of climate warming. The findings of Falarz (2019) partially support the results of the current study. In their study, Zhang et al. (2001) noted that the decrease in mean SLP caused by increasing SST led to an increase in the number of cyclones in the Icelandic low-pressure region. However, Edwards et al. (2022) stated that despite the positive changes in the NAO index from 2010 to 2020, no changes in the Icelandic low-pressure system have been observed, which aligns with the results of the present study. The expansion of the subtropical high-pressure system toward Western Europe and the strengthening of the Atlantic Ocean's trough in the spring (Figs. 3 and 4) indicate the intensification of the Atlantic storm track. The significant decrease in SLP, corresponding to the central Atlantic Ocean, serves as evidence for this claim. Eichler et al. (2014) investigated the changes in the intensity of the Atlantic storm track during winter, and their results are consistent with the current study's findings for this period. Regarding the multi-decade trend of annular modes (North Atlantic, NAM/NAO, and Pacific Ocean, NAM/NP), it has been observed that they just exhibited increased strength in the Pacific Ocean between 1922 and 1959, followed by a period of weakening from 1960 to 1985. Of particular importance is the positive trend observed in the NAM/NAO index from 1960 to the early 1990s, which subsequently reversed in trend during the 1990s (Gong et al., 2018). Our findings indicate that during winter, the Azores high-pressure system experienced a 1 hPa increase in its central pressure, while no significant change was detected in the Iceland low-pressure system (Li and Wang, 2003). Hence, the rise in the NAM/NAO index can be attributed to the intensification of the Azores high pressure.

4.4.3 The Pacific Ocean and Aleutian low

If we consider the strengthening and weakening of the Aleutian low in relation to temperature alone,

the result is that climate warming and the increase in atmosphere thickness have weakened the middle-level trough of the atmosphere, ultimately leading to a weakening of the surface low pressure. Consequently, this system has shown a significant positive trend in winter. The weakening of the Aleutian low pressure means the weakening of the Pacific storm track, as previously reported by McCabe et al. (2004), Wang et al. (2012), and Eichler et al. (2014). In relation to other forcing factors, Trenberth and Hurrell (1994) and Gan et al. (2016) proposed a linear model suggesting that the strengthening of the Aleutian low is a result of increased Bering SST and polar ice melting. However, Hoerling et al. (2001) and Gillett et al. (2005) argue that models cannot fully represent the complexity of the Aleutian low-SST relationship, as they only account for the response to SST while ignoring the unexplained effects of atmospheric internal variability. On the other hand, Bjerknes (1968), Horel and Wallace (1981), Hoerling et al. (2001), Branstator (2002), Lu et al. (2004), Xie et al. (2010), Deser et al. (2012), Oshima et al. (2012), Choi and Cha (2017), Tyrrell and Karpechko (2021), and Chen et al. (2023) also suggest that multiple drivers contribute to the uncertainty in the intensity of changes in the Aleutian low. Some of the drivers include Southeast Asia's stream jets, significant changes in the extratropical atmosphere, and teleconnection patterns. They state that despite climate warming, these factors can weaken the Aleutian low by creating anomalies in the atmospheric circulations of remote areas. Understanding the causes of observed changes in a system affected by various forcing factors is inherently challenging and complicated. For example, mean SST in the Pacific exhibits strong variations on time scales of 20-30 years (Boo et al., 2015). Wang et al. (2012) propose that large volcanic events and potentially the variability in incoming solar radiation contribute to determining the Pacific Decadal Oscillation (PDO) phase through changes in the Arctic Oscillation. Yeh et al. (2013) demonstrate that aerosols from anthropogenic sources can alter the temporal variability of the North Pacific SST through modifications to the atmospheric circulation. Some researchers have suggested that the variability in North Pacific SST is linked to local circulation changes in the Aleutian low (Latif and Barnett, 1996; Sun and Wang,

2006; Chen et al., 2020; Giamalaki et al., 2021; Dow et al., 2023). These suggestions strengthen the reliability of our research on the weakening of the Aleutian low pressure during its peak activity in winter. These results indicate that aerosols (both natural and anthropogenic) cool and increase SLP through radiant reflection, highlighting the dominant influence of aerosols on climate warming and the weakening of the Aleutian low. Yu and Kim (2011) studied the relationship between different phases of ENSO and SLP in extratropical regions and concluded that the warm phase of ENSO (El Niño) strengthens the Aleutian low pressure, and the cold phase has the opposite effect. According to the positive trends of the warm phases of ENSO (Yu and Kim 2011; Alizadeh, 2023), the strengthening of the Aleutian low pressure is expected, but with the results of this study and the weakening trend of this low pressure, it can be concluded that the impact of global warming on this low pressure is undeniable. However, further discussion and examination can be conducted in future studies.

The variability of the Annular Mode index over the Pacific Ocean (NPCI) indicates that it has experienced a substantial decrease since the 1950s, reaching its lowest value in the mid-1970s before gradually increasing until 2010. Gong et al. (2018) used a pattern-based index as NPCI, which is computed based on the empirical orthogonal function (EOF) modes of the winter mean of SLP anomalies over the North-Central Pacific. Therefore, despite the decrease in pressure in the Aleutian low region, it is expected that the NAM/PA as the first mode of variability over the Northern Pacific has become stronger in recent decades due to the influence of global warming.

4.4.4 Monsoon low

The factors influencing the formation of monsoons probably represent various responses to climate warming, resulting in the weakening or strengthening of monsoons at their main formation location. Sørland and Sorteberg (2015) and Dong et al. (2020) suggest that climate warming has led to a decrease in vorticity and a weakening of the monsoon low in its main core, which aligns with the present study's findings. Investigating changes in monsoon rainfall due to climate warming poses a significant challenge

as it involves internal natural variability, external natural forcing (e.g., solar and volcanic activity), and anthropogenic climatic factors (e.g., greenhouse gases, aerosols, and land use) (Wang. et al., 2013; Kamae et al., 2017). Moreover, the occurrence of monsoons results from changes in the direction of moist flow in tropical latitudes caused by weather system arrangements. Sukumaran and Ajayamohan (2014) propose that the changes in precipitation in the subcontinent are due to the displacement of the low-level jet (LLJ) flow, which has altered the path of moisture transport above 15º N. Additionally, they assert that the increase in atmospheric stability in the southern regions of the Arabian Sea (Rajendran et al., 2012; Sooraj et al. 2015) is also a consequence of the LLJ displacement. The rise in atmospheric temperature caused by climate warming over the cold ocean can explain the increased stability of the atmosphere in these areas, as observed in the study of Sooraj (2015). Kamae et al. (2017) demonstrated that since 1979, the trend of warming of the Atlantic and Indian oceans and cooling of the Pacific are related to the phase change of the multi-decadal oscillation of the Atlantic and the decadal oscillation of the Pacific.

4.4.5 Mediterranean region

In the Eastern Mediterranean, there is a significant positive trend during winter and autumn at the 500 hPa level, while a significant negative trend is observed during spring and summer at sea level. Similar findings have been reported by Aragão and Porcu (2022) and Kotsias et al. (2023). In the Western Mediterranean, a significant positive trend is observed at the 500 hPa level during spring, while a significant negative trend is observed at sea level during summer. Trigo et al. (2000) argue that there has been a decreasing trend in strong cyclones and an increasing trend in weak cyclones in the Western Mediterranean, which aligns with the observed trends. The results of this study on the Mediterranean (decreasing cyclones in the west and increasing cyclones in the east) are consistent with those of Maheras et al. (2001) and Nissen et al. (2013). These studies, along with the significance maps of sea level and atmospheric thickness indicating climate warming in recent decades, demonstrate the complexity of factors influencing cyclone formation in the Mediterranean, distinguishing it from other regions worldwide.

5. Summary and conclusions

The findings in this paper indicate significant positive trends in thickness maps across all seasons and a wide area of the Northern Hemisphere, thereby confirming the occurrence of climate warming in recent decades. These trends are particularly pronounced between latitudes 80º to 90º N and in subtropical regions. Notably, the increase in thickness resulting from heating is more prominent in mid-latitudes during the summer. While the presence of a significant and positive trend in atmospheric thickness within the Northern Hemisphere is an indicator of climate warming, its impacts on large-scale atmospheric systems and circulation patterns are distinctly varied. It is evident that the drivers influencing system formation undergo diverse effects due to climate warming, resulting in different and sometimes opposing conditions. Local and regional factors can exert such strong and influential roles that they render the activities of a phenomenon on a global scale ineffective or even neutral (e.g., the Siberian high). Although all the evidence presented in this study confirms the undeniable role of current warming in the increase of 500 hPa heights and thicknesses, the effects on continents and oceans have exhibited notable differences. To gain a more comprehensive understanding of these results, further extensive studies are required to identify more precise reasons. It is also suggested to investigate the role of atmospheric thickness and pressure changes on other meteorological parameters, such as precipitation, in future research studies.

References

Alizadeh O. 2023. A review of ENSO teleconnections at present and under future global warming. WIREs Climate Change 15: e861. https://doi.org/10.1002/wcc.861

Anscombe FJ, Tukey JW. 2012. The examination and analysis of residuals. Technometrics 5: 141-160. https://doi.org/10.1080/00401706.1963.10490071

Aragão L, Porcu F. 2022. Cyclonic activity in the Mediterranean region from a high-resolution perspective using ECMWF ERA5 dataset. Climate Dynamics 58: 1293-1310. https://doi.org/10.1007/s00382-021-05963-x

Banda V, Dzwairo B, Singh S, Kanyerere T. 2021. Trend analysis of selected hydro-meteorological variables for the Rietspruit sub-basin, South Africa. Journal of

Water and Climate Change 12: 3099-3123. https://doi.org/10.2166/wcc.2021.260

Bjerknes JAB. 1968. Atmospheric teleconnections from the Equatorial Pacific. RAND Corporation, 40 pp. Available at https://www.rand.org/pubs/papers/P3882.html

Boo KO, Booth BBB, Byun YH, Lee J, Cho C, Shim S, Kim KT. 2015. Influence of aerosols in multidecadal SST variability simulations over the North Pacific. Journal of Geophysical Research: Atmospheres 120: 517-531. https://doi.org/10.1002/2014JD021933

Branstator G. 2002. Circumglobal teleconnections, the jet stream waveguide, and the North Atlantic Oscillation. Journal of Climate 15: 1893-1910. https://doi.org/10.1175/1520-0442(2002)015<1893:CTTJSW>2.0.CO;2

Burt PJA. 2005. Book review: Climate change, causes, effects and solutions. By John T. Hardy Wiley, Chichester, 2003 xii + 247 pp. ISBN 0 470 85019 1. Weather 60: 301-301. https://doi.org/10.1256/wea.125.04

Castruccio FS, Ruprich-Robert Y, Yeager SG, Danabasoglu G, Msadek R, Delworth TL. 2019. Modulation of Arctic Sea ice loss by atmospheric teleconnections from Atlantic Multidecadal Variability. Journal of Climate 32: 1419-1441. https://doi.org/10.1175/JCLI-D-18-0307.1

Chen S, Chen W, Wu R, Yu B, Graf H-F. 2020. Potential impact of preceding Aleutian Low variation on the El Niño-Southern Oscillation during the following winter. Journal of Climate 33: 3061-3077. https://doi.org/10.1175/JCLI-D-19-0717.1

Chen S, Chen W, Yu B, Wu R, Graf H-F, Chen L. 2023. Enhanced impact of the Aleutian Low on increasing the Central Pacific ENSO in recent decades. Climate and Atmospheric Science 6: 1-13. https://doi.org/10.1038/s41612-023-00350-1

Choi J-W, Cha Y. 2017. Anomalous variation in summer tropical cyclone activity by preceding winter Aleutian low oscillation. Atmospheric Science Letters 18: 268-275. https://doi.org/10.1002/asl.752

Cohen JL, Entekhabi D. 1999. Eurasian snow cover variability and northern hemisphere climate predictability. Geophysical Research Letters 26: 345-348. https://doi.org/10.1029/1998GL900321

Cohen JL, Furtado JC, Barlow MA, Alexeev VA, Cherry JE. 2012. Arctic warming, increasing snow cover and widespread boreal winter cooling. Environmental Research Letters 7: 014007. https://doi.org/10.1088/1748-9326/7/1/014007

D'Arrigo R, Jacoby G, Wilson R, Panagiotopoulos F. 2005. A reconstructed Siberian High index since A. D. 1599 from Eurasian and North American tree rings. Geophysical Research Letters 32: L05705. https://doi.org/10.1029/2004GL022271

Deser C, Phillips A, Bourdette V, Teng H. 2012. Uncertainty in climate change projections: The role of internal variability. Climate Dynamics 38: 527-546. https://doi.org/10.1007/s00382-010-0977-x

Dong W, Lin Y, Wright J, Xie Y, Xu F, Xu W, Yan W. 2017. Indian monsoon low-pressure systems feed up-and-over moisture transport to the southwestern Tibetan plateau: Up-and-over moisture transport. Journal of Geophysical Research Atmospheres 122: 12,140-12,151. https://doi.org/10.1002/2017JD027296

Dong W, Ming Y, Ramaswamy V. 2020. Projected changes in South Asian monsoon low-pressure systems. Journal of Climate 33: 7275-7287. https://doi.org/10.1175/JCLI-D-20-0168.1

Dow WJ, McKenna CM, Joshi MM, Blaker A T, Rigby R, Maycock AC. 2023. Intensified Aleutian Low induces weak Pacific Decadal Variability. EGUsphere [preprint]. https://doi.org/10.5194/egusphere-2023-1595

Edwards M, Beaugrand G, Kléparski L, Hélaouët P, Reid PC. 2022. Climate variability and multi-decadal diatom abundance in the Northeast Atlantic. Communications Earth and Environment 3: 162. https://doi.org/10.1038/s43247-022-00492-9

Eichler P, Pimenta F, Eichler B, Vital H. 2014. Living *Bulimina marginata* in the SW Atlantic Continental margin: Effect of the subtropical shelf front and South Atlantic central water. Continental Shelf Research 89: 88-92. https://doi.org/10.1016/j.csr.2013.09.027

Falarz M. 2019. Azores High and Hawaiian High: Correlations, trends and shifts (1948-2018). Theoretical and Applied Climatology 138: 417-431. https://doi.org/10.1007/s00704-019-02837-5

Frimpong BF, Koranteng A, Molkenthin F. 2022. Analysis of temperature variability utilising Mann-Kendall and Sen's slope estimator tests in the Accra and Kumasi metropolises in Ghana. Environmental Systems Research 11: 24. https://doi.org/10.1186/s40068-022-00269-1

Fu Q, Johanson CM, Wallace JM, Reichler T. 2006. Enhanced mid-latitude tropospheric warming in satellite measurements. Science 312: 1179-1179. https://doi.org/10.1126/science.1125566

Fu Q, Lin P. 2011. Poleward shift of subtropical jets inferred from satellite-observed lower-stratospheric

temperatures. Journal of Climate 24: 5597-5603. https://doi.org/10.1175/JCLI-D-11-00027.1

Gadedjisso-Tossou A, Adjegan KI, Kablan A K M. 2021. Rainfall and temperature trend analysis by Mann-Kendall test and significance for rainfed cereal yields in northern Togo. Sci 3: 17. https://doi.org/10.3390/sci3010017

Gan B, Wu L, Jia F, Li S, Cai W, Nakamura H, Alexander M A, Miller A J. 2016. On the response of the Aleutian Low to greenhouse warming. Journal of Climate 30: 3907-3925. https://doi.org/10.1175/JCLI-D-15-0789.1

Gan TY. 1998. Hydroclimatic trends and possible climatic warming in the Canadian prairies. Water Resources Research 34: 3009-3015. https://doi.org/10.1029/98wr01265

Gascard JC, Zhang J, Rafizadeh M. 2019. Rapid decline of Arctic sea ice volume: Causes and consequences. The Cryosphere Discuss [preprint]. https://doi.org/10.5194/tc-2019-2

Giamalaki K, Beaulieu C, Henson SA, Martin AP, Kassem H, Faranda D. 2021. Future intensification of extreme Aleutian low events and their climate impacts. Scientific Reports 11: 18395. https://doi.org/10.1038/s41598-021-97615-7

Gibbons JD, Chakraborti S. 2011. Nonparametric statistical inference. In: International encyclopedia of statistical science (Lovric M., Ed.). Springer Berlin Heidelberg, 977-979. https://doi.org/10.1007/978-3-642-04898-2_420

Gillett NP, Allan RJ, Ansell T J. 2005. Detection of external influence on sea level pressure with a multi-model ensemble. Geophysical Research Letters 32: L19714. https://doi.org/10.1029/2005GL023640

Gong DY, Ho CH. 2002. The Siberian High and climate change over middle to high latitude Asia. Theoretical and Applied Climatology 72: 1-9. https://doi.org/10.1007/s007040200008

Gong H, Wang L, Chen W, Nath D. 2018. Multidecadal fluctuation of the wintertime Arctic Oscillation Pattern and its implication. Journal of Climate 31: 5595-5608. https://doi.org/10.1175/JCLI-D-17-0530.1

Hannigan A, Godek M. 2020. The utility of 1000-500 mb thickness and weather type as a rain-snow divide: A 30-year study at Albany, NY. Atmospheric and Climate Sciences 10: 372-391. https://doi.org/10.4236/acs.2020.103021

Hirsch R, Slack J, Smith R. 1982. Techniques of trend analysis for monthly water quality data. Water Resources Research 18: 107-121. https://doi.org/10.1029/WR018i001p00107

Hoerling MP, Hurrell JW, Xu T. 2001. Tropical origins for recent North Atlantic climate change. Science 292: 90-92. https://doi.org/10.1126/science.1058582

Horel J, Wallace J. 1981. Planetary-scale atmospheric phenomena associated with the Southern Oscillation. Monthly Weather Review 109: 813-829. https://doi.org/10.1175/1520-0493(1981)109<0813:PSAPAW>2.0.CO;2

Hunt K, Turner A, Inness P, Parker D, Levine R. 2016. On the structure and dynamics of Indian monsoon depressions. Monthly Weather Review 144: 3391-3416. https://doi.org/10.1175/MWR-D-15-0138.1

Hurley JV, Boos WR. 2015. A global climatology of monsoon low pressure systems. Quarterly Journal of the Royal Meteorological Society 141: 1049-1064. https://doi.org/10.1002/qj.2447

IPCC. 2021. Climate change 2021. The physical science basis. Contribution of Working Group I to the Sixth Assessment Report of the Intergovernmental Panel on Climate Change. Cambridge University Press, Cambridge, USA, 2391 pp. https://doi.org/10.1017/9781009157896

Jeong JH, Ou T, Linderholm H, Kim BM, Kim SJ, Kug J S, Chen D. 2011. Recent recovery of the Siberian High intensity. Journal of Geophysical Research 116: D23102. https://doi.org/10.1029/2011jd015904

Jiqin H, Gelata FT, Chaka Gemeda S. 2023. Application of MK trend and test of Sen's slope estimator to measure impact of climate change on the adoption of conservation agriculture in Ethiopia. Journal of Water and Climate Change 14: 977-988. https://doi.org/10.2166/wcc.2023.508.

Kamae Y, Li X, Xie SP, Ueda H. 2017. Atlantic effects on recent decadal trends in global monsoon. Climate Dynamics 49: 3443-3455. https://doi.org/10.1007/s00382-017-3522-3

Kay JE, Deser C, Phillips A, Mai A, Hannay C, Strand G, Vertenstein M. 2015. The Community Earth System Model (CESM) Large Ensemble Project: A community resource for studying climate change in the presence of internal climate variability. Bulletin of the American Meteorological Society 96: 1333-1349. https://doi.org/10.1175/BAMS-D-13-00255.1

Kotsias G, Lolis C, Hatzianastassiou N, Bakas N, Lionello P, Bartzokas A. 2023. Objective climatology and classification of the Mediterranean cyclones based on

the ERA5 data set and the use of the results for the definition of seasons. Theoretical and Applied Climatology 152: 1-17. https://doi.org/10.1007/s00704-023-04374-8

Latif M, Barnett TP. 1996. Decadal climate variability over the North Pacific and North America: Dynamics and predictability. Journal of Climate 9: 2407-2423. https://doi.org/10.1175/1520-0442(1996)009<2407:DCVOTN>2.0.CO;2

Li J, Wang JXL. 2003. A new North Atlantic Oscillation index and its variability. Advances in atmospheric sciences 20: 661-676. https://doi.org/10.1007/bf02915394

Lu J, Greatbatch RJ, Peterson KA. 2004. Trend in Northern Hemisphere winter atmospheric circulation during the last half of the twentieth century. Journal of Climate 17: 3745-3760. https://doi.org/10.1175/1520-0442(2004)017<3745:TINHWA>2.0.CO;2

Maheras P, Flocas H, Patrikas I, Anagnostopoulou C. 2001. A 40 year objective climatology of surface cyclones in the Mediterranean region: Spatial and temporal distribution. International Journal of Climatology 21: 109-130. https://doi.org/10.1002/joc.599

McCabe G, Palecki M, Betancourt J. 2004. Pacific and Atlantic Ocean influences on multidecadal drought frequency in the United States. Proceedings of the National Academy of Sciences of the United States of America 101: 4136-4141. https://doi.org/10.1073/pnas.0306738101

Mori M, Watanabe M, Shiogama H, Inoue J, Kimoto M. 2014. Robust Arctic sea-ice influence on the frequent Eurasian cold winters in past decades. Nature Geoscience 7 869-873. https://doi.org/10.1038/ngeo2277

Mori M, Kosaka Y, Watanabe M, Nakamura H, Kimoto M. 2019. A reconciled estimate of the influence of Arctic sea-ice loss on recent Eurasian cooling. Nature Climate Change 9: 123-129. https://doi.org/10.1038/s41558-018-0379-3

Nissen K, Leckebusch GC, Pinto J, Ulbrich U. 2013. Mediterranean cyclones and windstorms in a changing climate. Regional Environmental Change 14: 1873-1890. https://doi.org/10.1007/s10113-012-0400-8

NOAA/NWS N. 2019. Constant pressure charts: Thickness. National Oceanic and Atmospheric Administration/National Weather Service. Available at https://www.weather.gov/jetstream/thickness

Oshima K, Tanimoto Y, Xie SP. 2012. Regional patterns of wintertime SLP change over the North Pacific and their uncertainty in CMIP3 multi-model projections. Journal of the Meteorological Society of Japan 90A: 385-396. https://doi.org/10.2151/jmsj.2012-A23

Panagiotopoulos F, Shahgedanova M, Hannachi A, Stephenson DB. 2005. Observed trends and teleconnections of the Siberian High: A recently declining center of action. Journal of Climate 18: 1411-1422. https://doi.org/10.1175/JCLI3352.1

Patil SD, Singh HN, Bansod SD, Singh N. 2011. Trends in extreme mean sea level pressure and their characteristics during the summer monsoon season over the Indian region. International Journal of Remote Sensing 32: 701-715. https://doi.org/10.1080/01431161.2010.517793

Rajendran K, Kitoh A, Srinivasan J, Mizuta R, Krishnan R. 2012. Monsoon circulation interaction with Western Ghats orography under changing climate. Theoretical and Applied Climatology 110: 555-571. https://doi.org/10.1007/s00704-012-0690-2

Seidel DJ, Randel WJ. 2007. Recent widening of the tropical belt: evidence from tropopause observations. Journal of Geophysical Research Atmospheres 112: D20113. https://doi.org/10.1029/2007JD008861

Semenov VA, Park W, Latif M. 2009. Barents Sea inflow shutdown: A new mechanism for rapid climate changes. Geophysical Research Letters 36: L14709. https://doi.org/10.1029/2009GL038911

Sikka DR. 1977. Some aspects of the life history, structure and movement of monsoon depressions. Pure and Applied Geophysics 115: 1501-1529. https://doi.org/10.1007/BF00874421

Sooraj KP, Terray P, Mujumdar M. 2015. Global warming and the weakening of the Asian summer monsoon circulation: Assessments from the CMIP5 models. Climate Dynamics 45: 233-252. https://doi.org/10.1007/s00382-014-2257-7

Sørland SL, Sorteberg A. 2015. The dynamic and thermodynamic structure of monsoon low-pressure systems during extreme rainfall events. Tellus A: Dynamic Meteorology and Oceanography 67: 27039. https://doi.org/10.3402/tellusa.v67.27039

Sukumaran S, Ajayamohan R. 2014. Poleward shift in Indian Summer Monsoon low level jetstream under global warming. Climate Dynamics 45: 33-351. https://doi.org/10.1007/s00382-014-2261-y

Sun J, Wang H. 2006. Relationship between Arctic Oscillation and Pacific Decadal Oscillation on decadal timescale. Chinese Science Bulletin 51: 75-79. https://doi.org/10.1007/s11434-004-0221-3

Swart NC, Fyfe JC, Gillett N, Marshall GJ. 2015. Comparing trends in the Southern Annular Mode and Surface Westerly Jet. Journal of Climate 28: 8840-8859. https://doi.org/10.1175/JCLI-D-15-0334.1

Trenberth KE, Hurrell JW. 1994. Decadal atmosphere-ocean variations in the Pacific. Climate Dynamics 9: 303-319. https://doi.org/10.1007/BF00204745

Trigo IF, Davies TD, Bigg GR. 2000. Decline in Mediterranean rainfall caused by weakening of Mediterranean cyclones. Geophysical Research Letters 27: 2913-2916. https://doi.org/10.1029/2000GL011526

Tyrrell N, Karpechko A. 2021. Minimal impact of model biases on Northern Hemisphere El Niño-Southern Oscillation teleconnections. Weather and Climate Dynamics 2: 913-925. https://doi.org/10.5194/wcd-2-913-2021

Vicente-Serrano S, López-Moreno JI. 2006. The influence of atmospheric circulation at different spatial scales on winter drought variability through a semi-arid climatic gradient in northeast Spain. International Journal of Climatology 26: 1427-1453. https://doi.org/10.1002/joc.1387

Wallace JM, Fu Q, Smoliak BV, Lin P, Johanson CM. 2012. Simulated versus observed patterns of warming over the extratropical Northern Hemisphere continents during the cold season. Proceedings of the National Academy of Sciences 109: 14337-14342. https://doi.org/10.1073/pnas.1204875109

Wang B, Liu J, Kim HJ, Webster PJ, Yim SY, Xiang B. 2013. Northern Hemisphere summer monsoon intensified by mega-El Niño/Southern Oscillation and Atlantic Multidecadal Oscillation. Proceedings of the National Academy of Sciences 110: 5347-5352. https://doi.org/10.1073/pnas.1219405110

Wang P, Wang JXL, Zhi H, Wang Y, Sun X. 2012. Circulation indices of the Aleutian low pressure system: Definitions and relationships to climate anomalies in the northern hemisphere. Advances in Atmospheric Sciences 29: 1111-1118. https://doi.org/10.1007/s00376-012-1196-7

Wang T, Ottera OH, Gao Y, Wang H. 2012. The response of the North Pacific decadal variability to strong tropical volcanic eruptions. Climate Dynamics 39: 2917-2936. https://doi.org/10.1007/s00382-012-1373-5

Xie SP, Deser C, Vecchi GA, Ma J, Teng H, Wittenberg AT. 2010. Global warming pattern formation: Sea surface temperature and rainfall. Journal of Climate 23: 966-986. https://doi.org/10.1175/2009JCLI3329.1

Yeager SG, Karspeck AR, Danabasoglu G. 2015. Predicted slowdown in the rate of Atlantic sea ice loss. Geophysical Research Letters 42: 10,704-710,713. https://doi.org/10.1002/2015GL065364

Yeh SW, Kim WM, Kim YH, Moon BK, Park RJ, Song CK. 2013. Changes in the variability of the North Pacific sea surface temperature caused by direct sulfate aerosol forcing in China in a coupled general circulation model. Journal of Geophysical Research 118: 1261-1270. https://doi.org/10.1029/2012JD017947

Yu J, Kim ST. 2011. Relationships between extratropical sea level pressure variations and the Central Pacific and Eastern Pacific types of ENSO. Journal of Climate 24: 708-720. https://doi.org/10.1175/2010JCLI3688.1

Zhang T, Stamnes K, Bowling SA. 2001. Impact of the atmospheric thickness on the atmospheric downwelling longwave radiation and snowmelt under clear-sky conditions in the Arctic and Subarctic. Journal of Climate 14: 920-939. https://doi.org/10.1175/1520-0442(2001)014<0920:IOTATO>2.0.CO;2